

# Flagging and handling cellwise outliers by robust estimation of a covariance matrix

Jakob Raymaekers and Peter J. Rousseeuw  
Department of Mathematics, KU Leuven, Belgium

December 28, 2019

## Abstract

We propose a method for detecting cellwise outliers. Given a robust covariance matrix, outlying cells (entries) in a row are found by the cellFlagger technique which combines lasso regression with a stepwise application of constructed cutoff values. The  $L^1$  penalty of the lasso has a physical interpretation as the total distance that suspicious cells need to move in order to bring their row into the fold. For estimating a cellwise robust covariance matrix we construct a detection-imputation method which alternates between flagging outlying cells and updating the covariance matrix as in the EM algorithm. The proposed methods are illustrated by simulations and on real data about volatile organic compounds in children.

*Keywords:* anomalous cells, cellFlagger, detection-imputation method, least angle regression algorithm, weighted lasso.

## 1 Introduction

It is a fact of life that most real data sets contain outliers, that is, elements that do not fit in with the majority of the data. These outliers can be annoying errors, but may also contain valuable information. In either case, finding them is of practical importance. In statistics this is called outlier detection, and in the computer science literature it is also called anomaly detection or exception mining, see e.g. Chandola et al. (2009).

The most common paradigm is that of casewise outliers, which assumes that most cases were drawn from a certain model distribution but some other cases were not. The latter are also called rowwise outliers, since data often comes in the form of a table (matrix)

in which the rows are the cases and the columns represent the variables. In computer science one often uses outlier detection methods based on Euclidean distances, which by construction are invariant for orthogonal transformations of the rows. In statistics many outlier detection methods are also invariant for affine transformations, i.e. nonsingular linear transforms combined with shifts.

The study of cellwise outliers is a more recent research topic. This is the situation where some individual cells (entries) of the data matrix deviate from what they should have been. Alqallaf et al. (2009) first formulated this paradigm. Note that cells are intimately tied to the coordinate system, whereas orthogonal or other linear transformations would change the cells. To illustrate the difference between the rowwise and cellwise approaches, consider the standard multivariate Gaussian model in dimension  $d = 4$  with the suspicious point  $(10, 0, 0, 0)$ . By an orthogonal transformation of the data this point can be moved to  $(\sqrt{50}, \sqrt{50}, 0, 0)$  or to  $(5, 5, 5, 5)$  so any orthogonally invariant rowwise detection method will treat all three situations the same way. But in the cellwise paradigm  $(10, 0, 0, 0)$  has one outlying cell,  $(\sqrt{50}, \sqrt{50}, 0, 0)$  has two and  $(5, 5, 5, 5)$  has four.

For an illustration of cellwise outliers see Figure 1. It depicts part of a dataset that will be described later. The rows are cases and the columns are variables. The regular cells are shown in yellow. Red colored cells indicate that their value is higher than expected, while blue cells indicate unusually low values.

When the model has substantially correlated variables the cellwise outliers need not be marginally outlying, and then it can be quite hard to detect them. Van Aelst et al. (2011) proposed one of the first methods, based on an outlyingness measure of the Stahel-Donoho type. Farcomeni (2014) looks for the cells that, when put to missing, yield the highest Gaussian partial likelihood. Agostinelli et al. (2015) and Leung et al. (2017) use a univariate or bivariate filter on the variables to flag cellwise outliers, followed by S-estimation. Rousseeuw and Van den Bossche (2018) predict the values of all cells and flag the observed cells that differ much from their prediction. Debruyne et al. (2019) consider rowwise outliers and ask which variables contribute the most to their outlyingness. The O3 plot of Unwin (2019) visualizes cases that are outlying in lower dimensions.

There has also been substantial work to estimate the covariance matrix underlying the

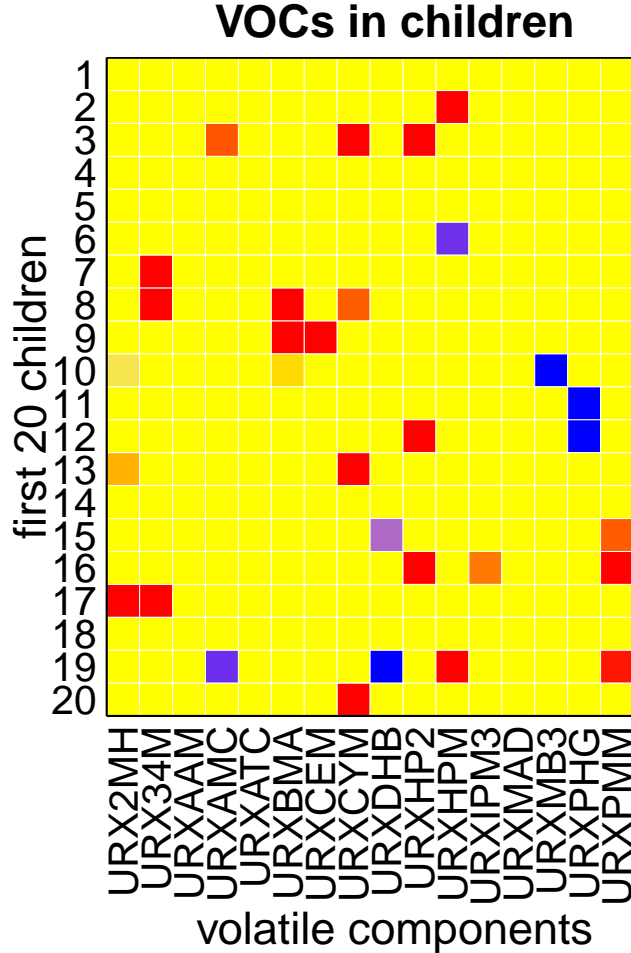


Figure 1: Illustration of cellwise outliers. Red squares indicate cells with unexpectedly high values, and blue squares indicate unusually low values. Regular cells are yellow.

model in the presence of cellwise outliers, which will be briefly reviewed in Section 3.1.

Most of the statistical research on cellwise outliers has focused on the FICM contamination model of Alqallaf et al. (2009) which assumes that the outlying cells come from a single distribution, and typically this distribution has all its mass in a single value  $\gamma$ . Here we will not restrict ourselves to that setting, and in the simulations we will allow for the cellwise outlying values to depend on which cells are contaminated, creating structured cellwise outliers. This is a more challenging problem, and it is clear that the underlying covariance structure will play a role. However, even if the pre-contamination covariance matrix  $\Sigma$  were known, no method is currently available to detect the cellwise outliers.

In Section 2 we will construct such a method, called cellFlagger. To estimate a cellwise

robust covariance matrix  $\widehat{\Sigma}$ , Section 3 constructs the detection-imputation algorithm which alternates between cellFlagger and re-estimating  $\Sigma$  as in the EM algorithm. In Section 4 the performance of this approach is studied by simulation, and Section 5 analyzes real data on volatile organic compounds in children.

## 2 The cellFlagger method

In this section we construct a method to detect outlying cells when the true covariance matrix is known. In reality that matrix is usually unknown, but this method is a major component of the algorithm proposed in the next section for estimating that matrix.

### 2.1 Ranking cells by their outlyingness

We start by standardizing the columns (variables) of the dataset, using robust univariate estimates of location and scale such as the median and the median absolute deviation. This also ensures that the result will be equivariant to shifting and rescaling of the original variables. The resulting  $d$ -variate cases are denoted as  $\mathbf{z}_i$  for  $i = 1, \dots, n$ .

For a given case  $\mathbf{z}$ , the central question in this section is how we can identify the cells that are most likely to be contaminated. Any set of cells in  $\mathbf{z}$  may be contaminated, and while it may be tempting to somehow investigate all  $2^d$  subsets of  $\mathbf{z}$  this quickly becomes infeasible due to the exponential complexity in  $d$ . Therefore we need a different approach to provide candidate cells that may be contaminated while avoiding an insurmountable computational cost. Note that the squared Mahalanobis distance  $\text{MD}^2(\mathbf{z}, \boldsymbol{\mu}, \Sigma) = (\mathbf{z} - \boldsymbol{\mu})' \Sigma^{-1} (\mathbf{z} - \boldsymbol{\mu})$  measures how far  $\mathbf{z}$  lies from the uncontaminated distribution. The idea is to reduce the Mahalanobis distance of  $\mathbf{z}$  by changing only a few cells. Mathematically, we look for a  $d$ -variate vector  $\boldsymbol{\delta}$  such that  $\text{MD}^2(\mathbf{z} - \boldsymbol{\delta}, \boldsymbol{\mu}, \Sigma)$  is small. Interestingly, this problem can be rewritten in an elegant form, as presented in the following proposition.

**Proposition 1.** *Modifying cells to reduce the Mahalanobis distance of their row can be rewritten using the sum of squares in a linear model.*

*Proof.* Observe that

$$\begin{aligned}
\text{MD}^2(\mathbf{z} - \boldsymbol{\delta}, \boldsymbol{\mu}, \boldsymbol{\Sigma}) &= (\mathbf{z} - \boldsymbol{\delta} - \boldsymbol{\mu})' \boldsymbol{\Sigma}^{-1} (\mathbf{z} - \boldsymbol{\delta} - \boldsymbol{\mu}) \\
&= \|\boldsymbol{\Sigma}^{-1/2}(\mathbf{z} - \boldsymbol{\delta} - \boldsymbol{\mu})\|_2^2 \\
&= \|\boldsymbol{\Sigma}^{-1/2}(\mathbf{z} - \boldsymbol{\mu}) - \boldsymbol{\Sigma}^{-1/2}\boldsymbol{\delta}\|_2^2 \\
&= \|\tilde{\mathbf{Y}} - \tilde{\mathbf{X}}\boldsymbol{\delta}\|_2^2
\end{aligned} \tag{1}$$

which is the objective of a regression without intercept with known response vector  $\tilde{\mathbf{Y}} := \boldsymbol{\Sigma}^{-1/2}(\mathbf{z} - \boldsymbol{\mu})$  and predictor matrix  $\tilde{\mathbf{X}} := \boldsymbol{\Sigma}^{-1/2}$  with coefficient vector  $\boldsymbol{\delta}$ .  $\square$

It is clear that the ordinary least squares (OLS) solution to (1) is  $\hat{\boldsymbol{\delta}}_{LS} = \mathbf{z} - \boldsymbol{\mu}$  since it makes the sum of squares zero. However, using  $\hat{\boldsymbol{\delta}}_{LS}$  would typically change all the cells of  $\mathbf{z}$  which is undesirable. We prefer to change as few cells as possible, so we want a sparse coefficient vector  $\hat{\boldsymbol{\delta}}$ . A natural choice for this problem is the lasso (Tibshirani, 1996), given by the minimization of

$$\|\tilde{\mathbf{Y}} - \tilde{\mathbf{X}}\boldsymbol{\delta}\|_2^2 + \lambda \|\boldsymbol{\delta}\|_1 \tag{2}$$

where  $\|\boldsymbol{\delta}\|_1 = |\delta_1| + \dots + |\delta_d|$ . Lasso regression penalizes  $\|\boldsymbol{\delta}\|_1$  which yields a path of sparse solutions to the regression problem for decreasing value of  $\lambda$ . Note that the penalty term  $\|\boldsymbol{\delta}\|_1$  has a concrete physical meaning in this setting: it is the total distance which the corresponding cells of  $\mathbf{z}$  need to travel in order to bring  $\mathbf{z}$  into the fold. This is unusual, as the  $L^1$  term is typically included as a device to induce sparsity without a specific subject-matter interpretation.

The method as described so far works fine for moderately outlying cells, but fails when some cells  $z_j$  lie far away. This is because moving them into place requires large components  $\delta_j$  which inflate the penalty term, so these  $z_j$  appear rather late in the lasso path. However, such marginal outliers  $z_j$  are easy to spot, as they have a large univariate outlyingness  $O_j = |z_j - \mu_j|/\sqrt{\Sigma_{jj}}$ . Therefore we downweight the  $\delta_j$  in the penalty term by a factor  $w_j = \min(1, 1.5/O_j)$  which is the weight associated with the univariate Huber M-estimator. This replaces the  $L^1$  norm in (2) by  $\|\mathbf{W}\boldsymbol{\delta}\|_1$  where  $\mathbf{W} := \text{diag}(w_1, \dots, w_d)$ . Note that this weighted lasso can be rewritten as a plain lasso as follows. Since all the weights are strictly positive  $\mathbf{W}$  is invertible, so we can write  $\tilde{\mathbf{X}}\boldsymbol{\delta} = (\tilde{\mathbf{X}}\mathbf{W}^{-1})(\mathbf{W}\boldsymbol{\delta}) = \dot{\mathbf{X}}\boldsymbol{\beta}$  where

$\dot{\mathbf{X}} := \tilde{\mathbf{X}}\mathbf{W}^{-1}$  and  $\boldsymbol{\beta} := \mathbf{W}\boldsymbol{\delta}$ . This merely changes the units of the variables in  $\tilde{\mathbf{X}}$ , yielding the minimization of

$$||\tilde{\mathbf{Y}} - \dot{\mathbf{X}}\boldsymbol{\beta}||_2^2 + \lambda||\boldsymbol{\beta}||_1 \quad (3)$$

followed by transforming  $\hat{\boldsymbol{\beta}}$  back to  $\hat{\boldsymbol{\delta}}$ . The penalty term  $||\boldsymbol{\beta}||_1$  keeps its interpretation in the new units determined by the  $w_j$ .

Note that lasso steps do not only add variables: sometimes they take a variable out of the model. But in our context it is natural to impose that once a cell is flagged it stays flagged, i.e. that a selected regressor stays in the model. By imposing this constraint we arrive at the elegant and fast least angle regression (LAR) algorithm of Efron et al. (2004). This is the option *type="lar"* in the R-package *lars* (Hastie and Efron, 2015), and its performance turned out to be very similar to that of *type="lasso"* in our setting. Using LAR also simplifies and speeds up the next step of cellFlagger in Section 2.2.

The way LAR works in our problem is intuitive. The gradient of  $\text{MD}^2(\mathbf{z} - \boldsymbol{\delta}, \boldsymbol{\mu}, \boldsymbol{\Sigma}) = ||\tilde{\mathbf{Y}} - \dot{\mathbf{X}}\boldsymbol{\beta}||_2^2$  with respect to  $\boldsymbol{\beta}$  is  $\boldsymbol{\nabla} = -2\dot{\mathbf{X}}'(\tilde{\mathbf{Y}} - \dot{\mathbf{X}}\boldsymbol{\beta})$ . This gradient  $\boldsymbol{\nabla} = (\nabla_1, \dots, \nabla_d)$  is zero at the minimum of  $\text{MD}^2$ , i.e. when  $\boldsymbol{\beta}$  is the OLS fit  $(\dot{\mathbf{X}}'\dot{\mathbf{X}})^{-1}\dot{\mathbf{X}}'\tilde{\mathbf{Y}} = \mathbf{W}(\mathbf{z} - \boldsymbol{\mu})$ . LAR first takes the coordinate with highest  $|\nabla_j|$  and moves  $\beta_j$ , i.e. cell  $j$ , to reduce  $|\nabla_j|$  until it equals the second largest  $|\nabla_h|$ . Then it moves cells  $j$  and  $h$  such that  $|\nabla_j| = |\nabla_h|$  decrease together, until it reaches the third largest  $|\nabla_m|$ , and so on.

For each row  $\mathbf{z}$  we have now obtained a ranking of its cells, corresponding to the order in which they occurred in the path for reducing  $\text{MD}^2(\mathbf{z} - \boldsymbol{\delta}, \boldsymbol{\mu}, \boldsymbol{\Sigma})$ .

## 2.2 Handling outlying cells

After  $k$  steps of LAR we have a set of  $k$  candidate cells. The question is whether these candidate cells are sufficient. In other words, is it possible to edit these  $k$  cells while keeping the remaining  $d - k$  cells intact, in such a way that the edited row behaves like a clean row? To this end we will edit the  $k$  candidate cells to maximize the Gaussian likelihood given the remaining cells. Suppose w.l.o.g. that the candidate cells are the first  $k$  entries of  $\mathbf{z}$  so we can write  $\mathbf{z}' = [\mathbf{z}'_1 \mathbf{z}'_2]$  and  $\boldsymbol{\mu}' = [\boldsymbol{\mu}'_1 \boldsymbol{\mu}'_2]$  where  $\mathbf{z}'_1$  and  $\boldsymbol{\mu}'_1$  have length  $k$ . Also write  $\boldsymbol{\Sigma}_{11}$  for the upper left submatrix of  $\boldsymbol{\Sigma}$  of size  $k \times k$  and so on. As in the E step of the EM algorithm (see e.g. Little and Rubin (1987)), maximizing the Gaussian likelihood

implies that  $\mathbf{z}_1$  should be shifted to  $E_{\boldsymbol{\mu}, \boldsymbol{\Sigma}}[\mathbf{Z}_1 | \mathbf{Z}_2 = \mathbf{z}_2] = \boldsymbol{\mu}_1 + \boldsymbol{\Sigma}_{12} \boldsymbol{\Sigma}_{22}^{-1}(\mathbf{z}_2 - \boldsymbol{\mu}_2)$ .

This imputation appears to require inverting the submatrix  $\boldsymbol{\Sigma}_{22}$  of  $\boldsymbol{\Sigma}$ . However, it can also be obtained by OLS regression in the model (1) of Proposition 1 but restricted to the set of  $k$  candidate variables. This is shown in the following proposition, the proof of which is given in Section A.1 of the Supplementary Material.

**Proposition 2.** *Let the  $k$ -variate  $\hat{\boldsymbol{\theta}}_1$  be the OLS fit to the regression problem given by*

$$\operatorname{argmin}_{\boldsymbol{\theta}} \|\boldsymbol{\Sigma}^{-1/2}(\mathbf{z} - \boldsymbol{\mu}) - (\boldsymbol{\Sigma}^{-1/2})_{\cdot 1} \boldsymbol{\theta}_1\|_2^2$$

where  $(\boldsymbol{\Sigma}^{-1/2})_{\cdot 1}$  denotes the first  $k$  columns of the matrix  $\boldsymbol{\Sigma}^{-1/2}$ . Then

$$\mathbf{z}_1 - \hat{\boldsymbol{\theta}}_1 = \boldsymbol{\mu}_1 + \boldsymbol{\Sigma}_{12} \boldsymbol{\Sigma}_{22}^{-1}(\mathbf{z}_2 - \boldsymbol{\mu}_2) \ .$$

In the implementation of cellFlagger these vectors  $\hat{\boldsymbol{\theta}}_1$  are obtained as a byproduct of the LAR algorithm without extra computational cost, see Section A.3. This means that it carries out the above computation for  $k = 1, \dots, d$  without having to invert any matrix.

We now have a sequence of length  $d$  of cells in  $\mathbf{z}$ , with their possible imputations at every stage  $k$ . The question remains where to stop in this path, i.e. how many cells should we actually flag? For that we use the following proposition:

**Proposition 3.** *For every  $1 \leq k \leq d$  we have:*

1. *The residual sum of squares  $RSS_k = \|\boldsymbol{\Sigma}^{-1/2}(\mathbf{z} - \boldsymbol{\mu}) - (\boldsymbol{\Sigma}^{-1/2})_{\cdot 1} \hat{\boldsymbol{\theta}}_1\|_2^2$  of the OLS fit  $\hat{\boldsymbol{\theta}}_1$  to the first  $k$  cells in the path equals the squared partial Mahalanobis distance  $MD^2(\mathbf{z}_2, \boldsymbol{\mu}_2, \boldsymbol{\Sigma}_{22}) = (\mathbf{z}_2 - \boldsymbol{\mu}_2)' \boldsymbol{\Sigma}_{22}^{-1}(\mathbf{z}_2 - \boldsymbol{\mu}_2)$ .*
2. *For Gaussian data the difference between two subsequent RSS follows the  $\chi^2$  distribution with 1 degree of freedom, i.e.  $\Delta_k := RSS_{k-1} - RSS_k \sim \chi^2(1)$ .*

The proof is in Section A.2 of the Supplementary Material. Following the path for  $1 \leq k \leq d$  we compare the  $\Delta_k$  to a cutoff  $q$ , say the 0.99 quantile of  $\chi^2(1)$ , and flag the cells with  $\Delta_k > q$ .

We illustrate cellFlagger by two simple bivariate examples. The left part of Figure 2 assumes that the true  $\boldsymbol{\mu} = \mathbf{0}$  and that  $\boldsymbol{\Sigma}$  is the identity matrix, so the correlation  $\rho$  is

zero. For any point  $\mathbf{z} = [z_1 \ z_2]'$  we can then run cellFlagger to see which of these cells are flagged, if any. In the central square no cells are flagged, to its left and right  $z_1$  is flagged, above and below it  $z_2$  is flagged, and in the outer regions both  $z_1$  and  $z_2$  are flagged. Things get more eventful when  $\Sigma$  has 1 on the diagonal and  $\rho = 0.9$  elsewhere. In the right panel of Figure 2 we see that no cells are flagged when  $\mathbf{z}$  lies in part of an elliptical region. The domain where only  $z_1$  is flagged now has a more complicated form, and the same holds for  $z_2$ , whereas the region in which both are flagged is similar to before. Of course the main purpose of cellFlagger is to deal with higher dimensions, which are harder to visualize.

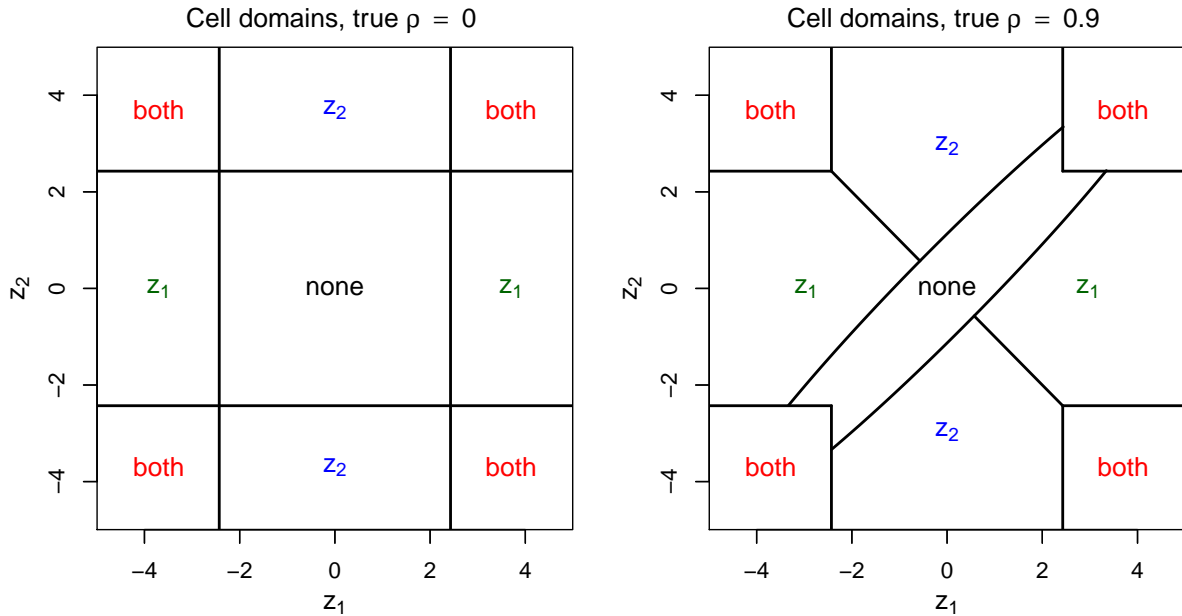


Figure 2: Bivariate domains where no cells are flagged, where only  $z_1$  is flagged, where only  $z_2$  is flagged, and where both are flagged, when the true correlation is  $\rho = 0$  (left panel) and when  $\rho = 0.9$  (right panel).

## 2.3 Simulation

To evaluate the performance of cellFlagger we run a small simulation in which the uncontaminated data are  $d$ -variate Gaussian with  $\boldsymbol{\mu} = \mathbf{0}$ . Since cellwise methods are neither affine or orthogonal invariant, we consider underlying covariance matrices  $\Sigma$  of two types. Type ALYZ are the randomly generated correlation matrices of Agostinelli et al. (2015)



which typically have relatively small correlations. Type A09 is given by  $\Sigma_{jh} := (-0.9)^{|j-h|}$  and contains both large and small correlations.

The outlying cells are generated as follows. The positions of the cells to be contaminated are obtained by randomly drawing  $n\varepsilon$  indices in each column of the data matrix. Then we look at each row  $(z_1, \dots, z_d)$  with such cells, and denote the indices of those cells as the set  $K = \{j(1), \dots, j(k)\}$  of size  $k$ . Next, we replace  $(z_{j(1)}, \dots, z_{j(k)})$  by the  $k$ -dimensional row  $\mathbf{v} = \gamma\sqrt{k}\mathbf{u}'/\text{MD}(\mathbf{u}, \boldsymbol{\mu}_K, \boldsymbol{\Sigma}_K)$  where  $\boldsymbol{\mu}_K$  and  $\boldsymbol{\Sigma}_K$  are restricted to the indices in  $K$  and where  $\mathbf{u}$  is the eigenvector of  $\boldsymbol{\Sigma}_K$  with smallest eigenvalue. This procedure generates  $\mathbf{v}$  which are structurally outlying in the subspace of the coordinates in  $K$ , while many of these cells will not be marginally outlying. This produces cellwise outliers that are more challenging than in the earlier literature, which used  $\mathbf{v} = (\gamma, \dots, \gamma)$ .

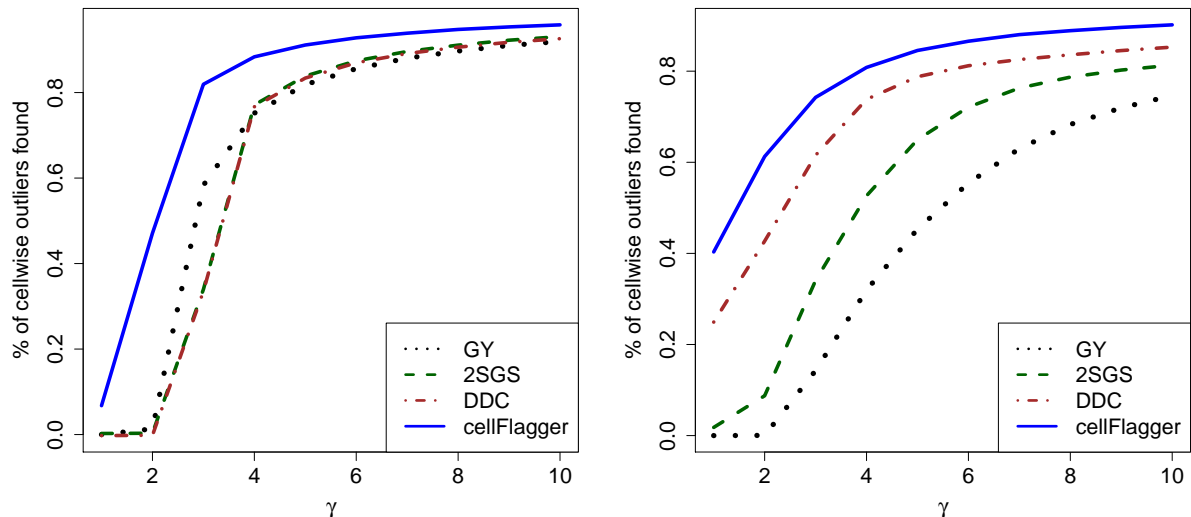


Figure 3: Percentage of cellwise outliers found for  $\Sigma_{\text{ALYZ}}$  (left) and  $\Sigma_{\text{A09}}$  (right).

Figure 3 shows the performance of cellFlagger in  $d = 20$  dimensions with  $\varepsilon = 10\%$  of cellwise outliers, using the covariance matrix estimated by the algorithm DDCW.DI described in Section 3.2. The other curves are from three existing techniques for flagging cells. The first one is the univariate Gervini-Yohai filter (GY) specified in (Agostinelli et al., 2015). The second is the multivariate DetectDeviatingCells (DDC) algorithm of Rousseeuw and Van den Bossche (2018), available in the `cellwise` package (Raymaekers et al., 2019). The third is the default filter of the 2SGS method in (Leung et al., 2017), which is a combination of a bivariate GY filter with DDC. We see that cellFlagger finds more of the

outlying cells at each  $\gamma$ . When  $\gamma$  increases the cellwise outliers become marginally outlying, making them easier to flag.

### 3 Cellwise robust estimation of a covariance matrix

#### 3.1 Existing approaches

The previous section described a method for flagging cellwise outliers when the true center  $\boldsymbol{\mu}$  and covariance matrix  $\boldsymbol{\Sigma}$  are known. Of course these are rarely known in practice, so they have to be estimated. The center  $\boldsymbol{\mu}$  can be estimated quite easily by applying a robust estimator (like the median) to each coordinate. Estimating the covariance matrix  $\boldsymbol{\Sigma}$  is the hard part. There exist several approaches to this problem.

A popular technique is to compute robust covariances between each pair of variables, and to assemble them in a matrix. To estimate these pairwise covariances, Öllerer and Croux (2015) and Croux and Öllerer (2016) use rank-based methods such as the Spearman and normal scores correlations. Tarr et al. (2016) instead propose to use the robust pairwise correlation estimator of Gnanadesikan and Kettenring (1972) in combination with the robust scale estimator  $Q_n$  of Rousseeuw and Croux (1993). As the resulting matrix is not necessarily positive semidefinite (PSD), they then compute the nearest PSD matrix by the algorithm of Higham (2002). All of these pairwise covariance estimators are fast to compute. We will compare the performance of these methods in Section 4.

A second approach is the snipEM procedure proposed by Farcomeni (2014) and implemented in the R package `snipEM` of Farcomeni and Leung (2019). Its first step flags cellwise outliers in each variable separately using a boxplot rule, and then "snips" them, which means making them missing. The second step tries many interchanges that unsnippet a randomly chosen snipped cell and at the same time snip a randomly chosen unsnippeted cell, and only keeps an interchange when it increases the partial Gaussian likelihood. This procedure is slower than the pairwise covariance approach.

The current state of the art to deal with complex cellwise outliers is the two-step generalized S-estimator (2SGS) of Agostinelli et al. (2015) and Leung et al. (2017) implemented in the R package `GSE` (Leung et al., 2019). In a first step, the method uses a filter (called

2SGS in Figure 3 above) to detect cellwise outliers. These cells are then set to missing, and the generalized S-estimator of Danilov et al. (2012) is run. A short survey of cellwise robust covariance estimators can be found in Sections 6.13 and 6.14 of Maronna et al. (2019).

### 3.2 The detection-imputation algorithm

Our algorithm for constructing a cellwise robust covariance matrix starts by standardizing the columns of the dataset as in the beginning of Section 2.1. Next, we compute initial estimators  $\hat{\boldsymbol{\mu}}^0$  and  $\hat{\boldsymbol{\Sigma}}^0$ . For this we can use the 2SGS estimator of Leung et al. (2017) described above. We will also try a different initial estimator called DDCW, which is a combination of the DDC method (Rousseeuw and Van den Bossche, 2018) and the wrapped covariance matrix of Raymaekers and Rousseeuw (2019). This initial estimator is described in Section A.4 of the Supplementary Material.

The detection-imputation (DI) algorithm then alternates the D-step and the I-step, both described below.

#### D-step: detecting outlying cells across all rows.

The D-step first applies the cellFlagger method of Section 2 to each row  $\mathbf{z}'_i$  based on the estimates  $\hat{\boldsymbol{\mu}}^{t-1}$  and  $\hat{\boldsymbol{\Sigma}}^{t-1}$  from the previous iteration step. This way each row  $\mathbf{z}'_i$  gets a ranking of its cells  $z_{ij}$ . From the  $\Delta_k$  in its path we construct a nonincreasing sequence of criterion values  $C_{ij} := \max_{h \geq k(j)} \Delta_h$ . If any cells  $z_{ih}$  are missing (NA) these are put in front of the path with  $C_{ih} := +\infty$ .

Should some columns have too many flagged cells (including NA's) it could become difficult to estimate a correlation between them, especially if the flagged sets overlap little. Even worse, flagging all cells in a column would remove all information about that variable. Therefore, we impose a maximal number of flagged cells in each column, including the NA's. This number is  $n \text{ maxCol}$  where the input parameter *maxCol* is set to 25% by default. Note that this is a constraint on the columns, whereas we are flagging cells by row. We resolve this with the following algorithm:

- sort the criterion values  $C_{ij}$  of all cells in the matrix in decreasing order;
- walk down this list. If a  $C_{ij}$  lies below the cutoff value  $q$  we “lock” row  $i$ , i.e. no cells of row  $i$  can be flagged any more. If  $C_{ij} > q$  the cell is flagged, unless it belongs to a column

which already has  $n \maxCol$  flagged cells. In the latter case, row  $i$  is locked also.

This procedure yields a (possibly empty) list of flagged cells in each row, which overall contains the most outlying cells subject to the  $\maxCol$  constraint.

### **I-step: Re-estimate $\mu$ and $\Sigma$ .**

The I-step is basically one step of the EM algorithm which considers the flagged cells as missing. However, it is computationally more efficient since it reuses results that are already available. In each row, the set of flagged cells is one of the active sets considered by LAR in cellFlagger, so its coefficient  $\hat{\theta}_1$  from Proposition 2 is known. This makes it trivial to impute the flagged cells, so the E-step of EM requires no additional computation. Next,  $\hat{\mu}^t$  and  $\hat{\Sigma}^t$  are computed as in the M-step, as described in more detail in Section A.5.

This iterative procedure stops when the Kullback-Leibler divergence (KLdiv) of  $\hat{\Sigma}^t$  from  $\hat{\Sigma}^{t-1}$  is below a tolerance, say 0.01. The KLdiv of an estimate  $\hat{\Sigma}_2$  from  $\hat{\Sigma}_1$  is defined as

$$\text{KLdiv}(\hat{\Sigma}_2, \hat{\Sigma}_1) = \text{trace}(\hat{\Sigma}_2 \hat{\Sigma}_1^{-1}) - \log(\det(\hat{\Sigma}_2 \hat{\Sigma}_1^{-1})) - d. \quad (4)$$

At the end of the DI algorithm we unstandardize  $\hat{\mu}$  and  $\hat{\Sigma}$  using the univariate location and scale estimates of the original data columns.

The time complexity of the DI algorithm is  $O(Tnd^3)$  where  $T$  is the number of iteration steps. This is the same complexity as that of the classical EM algorithm for covariance estimation with missing data.

## **4 Simulation results**

We simulate the estimators of covariance matrices discussed in the previous section. The data is generated as in Subsection 2.3, with dimensions  $d = 10, 20$  and  $40$ . The fraction of contaminated cells is  $\varepsilon = 0.1, 0.2$  in which  $\gamma$  varies from 1 to 10. In each replication we compute the Kullback-Leibler divergence (4) of the estimate  $\hat{\Sigma}$  from the underlying  $\Sigma$ , and then average the KLdiv over all replications. We show the results for  $\varepsilon = 0.2$ , since this is the most challenging scenario. The results for  $\varepsilon = 0.1$  were qualitatively similar.

Figure 4 compares the proposed methods to the existing approaches described in Subsection 3.1, for  $d = 10$ . Since  $\varepsilon = 0.2$  there are on average two cellwise outliers per row.

Gaussian rank (Grank) and Spearman refer to the covariance matrices of Öllerer and Croux (2015) and Croux and Öllerer (2016) using those rank correlations. The Gnanadesikan-Kettenring procedure of Tarr et al. (2016) is labeled GKnpd. Next, the snipEM method of Farcomeni (2014) and the 2SGS estimator of Leung et al. (2017) are plotted. The method 2SGS.DI uses 2SGS as initial estimator followed by the new DI method of Section 3.2. Also the initial estimator DDCW described in Section A.4 is shown, as well as DI applied to it.

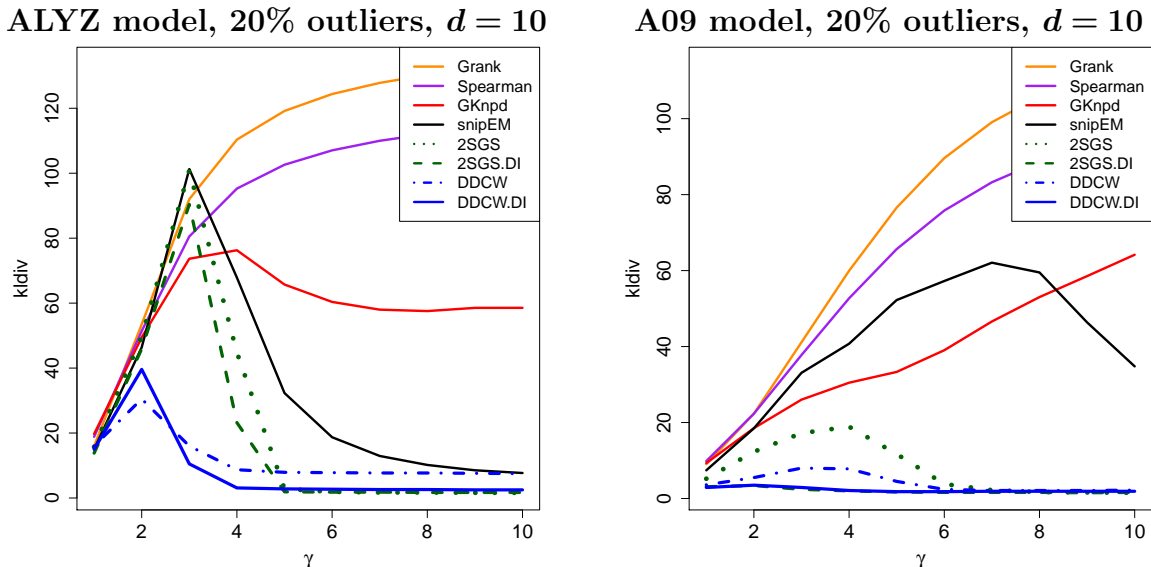


Figure 4: Kullback-Leibler divergence of covariance matrices for  $d = 10$  and  $n = 100$ .

We see that the three pairwise methods Grank, Spearman and GKnpd pay for their fast computation by a high KLdiv. The snipEM method does better for high  $\gamma$ , in part because the boxplot rule in its first step snips marginally outlying cells. The three pairwise methods do not use such a rule to flag marginally outlying cells, so high  $\gamma$  values impact them more. The state of the art method 2SGS does substantially better, and is improved by applying DI to it, both in the ALYZ and A09 models. The same holds for DDCW and DDCW.DI. Note that DI improves the results more under A09 than ALYZ, because A09 has bigger correlations so DI has more opportunities to make a difference.

We now consider higher dimensions, starting with  $d = 20$  in the top panels of Figure 5. The curves of Grank, Spearman, GKnpd and snipEM were much higher in this case, so we only show the four best performing methods in order to see the differences between them. Also here the DI algorithm substantially improves upon the initial estimators. The

improvement is largest under A09 which contains some high correlations. For  $d = 40$  (bottom panels) we see similar patterns.

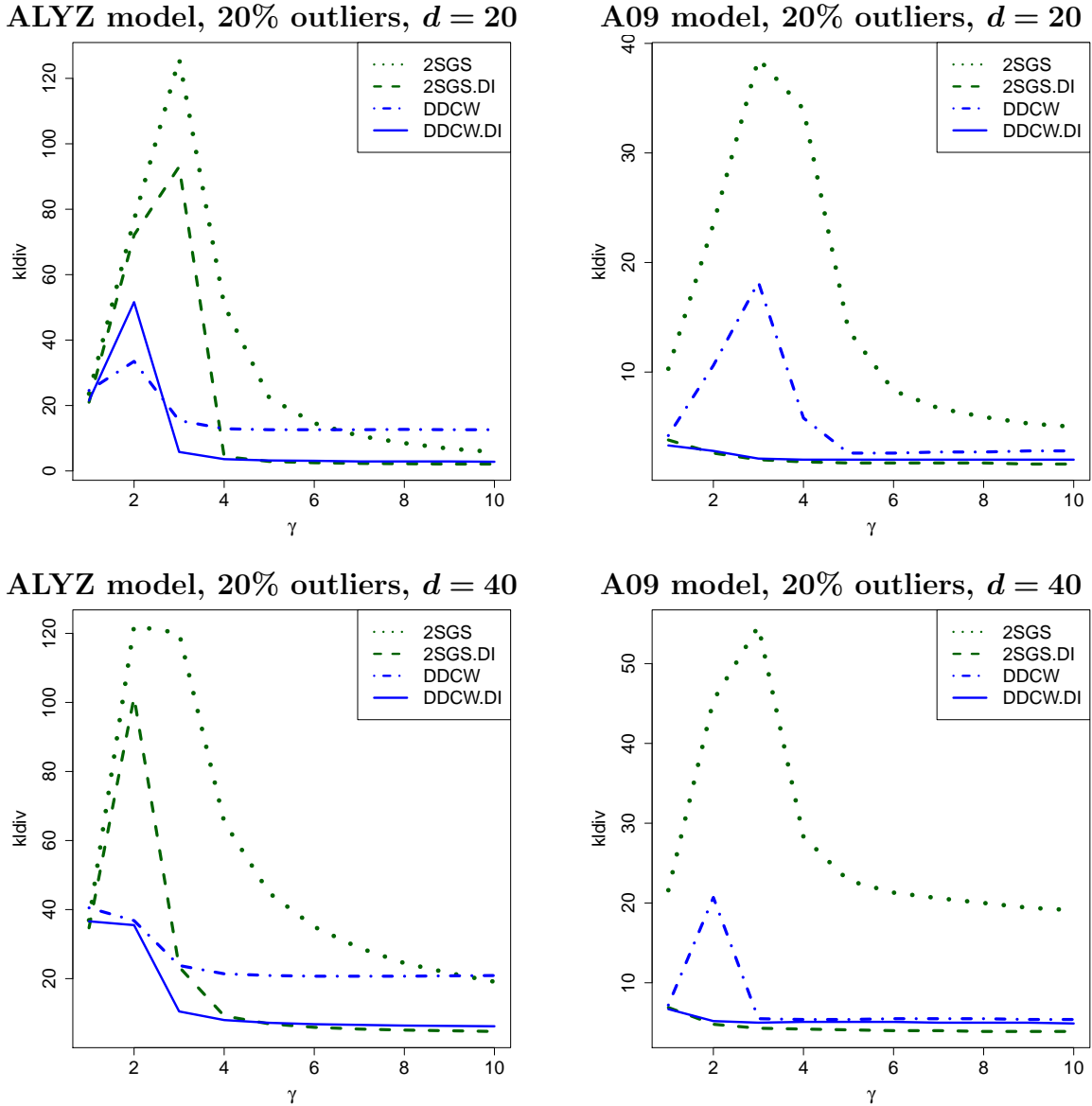


Figure 5: Kullback-Leibler divergence of covariance matrices for  $d = 20$  and  $n = 400$  (top panels) and for  $d = 40$  and  $n = 800$  (bottom panels).

Section A.6 of the Supplementary Material shows the results of a simulation in which the data are contaminated by 10% of cellwise outliers generated as above, plus 10% of rowwise outliers. In this particular setting "rowwise outliers" refers to rows in which all cells are contaminated in the same way as before, that is, rows with  $d$  cellwise outliers.

The initial estimators 2SGS and DDCW attempt to downweight or discard such rows. The results are qualitatively similar to those in Figures 4 and 5.

## 5 Example: volatile organic compounds in children

We study a dataset of volatile organic compounds (VOCs) in human urinary samples. The data was taken from the publicly available website of the National Health and Nutrition Examination Survey (NHANES, 2019), using the most recent available epoch. Such VOC metabolites are commonly monitored since chronic exposure to high levels of some VOCs can lead to a number of health problems such as cancer and neurocognitive dysfunction. The original dataset consists of 29 VOC metabolites, but we focus on a subset of 16 variables obtained by removing columns with a lot of missing values and/or zero median absolute deviation. Section A.7 in the Supplementary Material contains a table with the VOCs analyzed. In order to obtain a relatively homogeneous subset, we selected the data for children aged 10 or younger. The final dataset contained 512 subjects. We log-transformed the concentrations to make the variables roughly Gaussian (apart from possible outliers).

We estimated the covariance matrix of the data by the DI algorithm, starting from the DDCW initial estimator. The algorithm converged after 7 steps. Using the resulting covariance estimate we ran the cellFlagger algorithm with cutoff  $\sqrt{\chi^2_{1,0.99}} \approx 2.57$  to detect outlying cells. The corresponding cellmap of the first 20 children in the list was shown as Figure 1 in the introduction. Each row of the cellmap corresponds to a child, with inlying cells colored yellow. Red colored cells indicate that their value is higher than predicted given the inlying cells of that row, while blue cells indicate lower than predicted values. The more extreme the residual, the more intense the color.

One variable that stood out was URXCYM (N-Acetyl-S-(2-cyanoethyl)-L-cysteine) in which cellFlagger indicated 11% of large cell residuals. This was particularly striking since that variable had fewer than 2% of marginal outliers using the same cutoff  $\sqrt{\chi^2_{1,0.99}}$  on the absolute standardized values, and these were rather nearby (note that even for perfectly Gaussian data there would already be 1% of absolute standardized values above this cutoff). Figure 6 plots the cell residuals (which are zero for cells that were not flagged) versus the robustly standardized marginal values, with the cutoffs indicated by horizontal and vertical

lines. Most of the outlying cellwise residuals correspond to inlying marginal values. These children have extreme URXCYM values relative to their other VOCs.

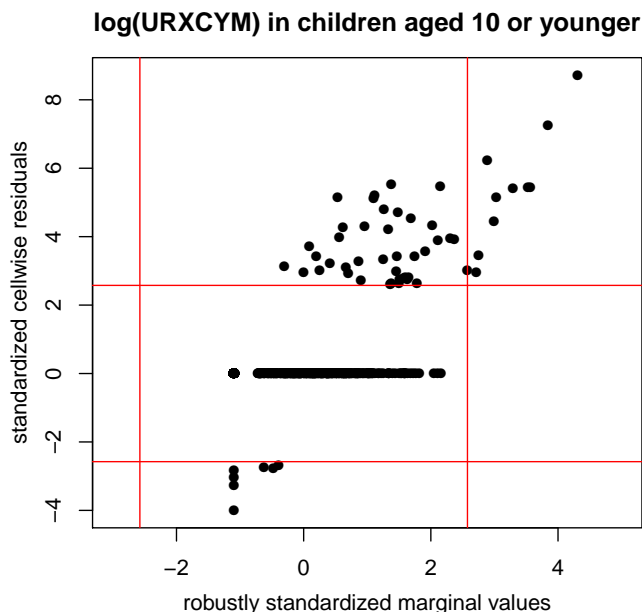


Figure 6: Plot of standardized cell residuals of  $\log(\text{URXCYM})$  obtained by cellFlagger, versus the robustly standardized values of  $\log(\text{URXCYM})$  on its own.

Interestingly, URXCYM is a well known biomarker for identifying smokers among adults, see e.g. Chen et al. (2019), since it typically results from the metabolization of acrylonitrile, a volatile liquid present in tobacco smoke. But in this example we are studying children, who are not supposed to smoke. In search of an explanation we combined the VOC data with the questionnaire data available on the same website (NHANES, 2019). Among many other things, these data contain information on the smoking status of the adults (usually parents) in the same household. These fell into four categories: only non-smoking adults, smoking adults who do not smoke inside the home, one adult smoking in the home, and two adults smoking in the home. The blue curve in Figure 7 shows the percentage of children with URXCYM cell residuals above the cutoff, in each of these categories. They go from 4.7% in households with only nonsmoking adults up to 72.7% in homes where two adults smoke, indicating that passive smoking has a measurable effect on children. On the other hand, if we were to look only at the marginal URXCYM values (red curve) no such effect is visible.



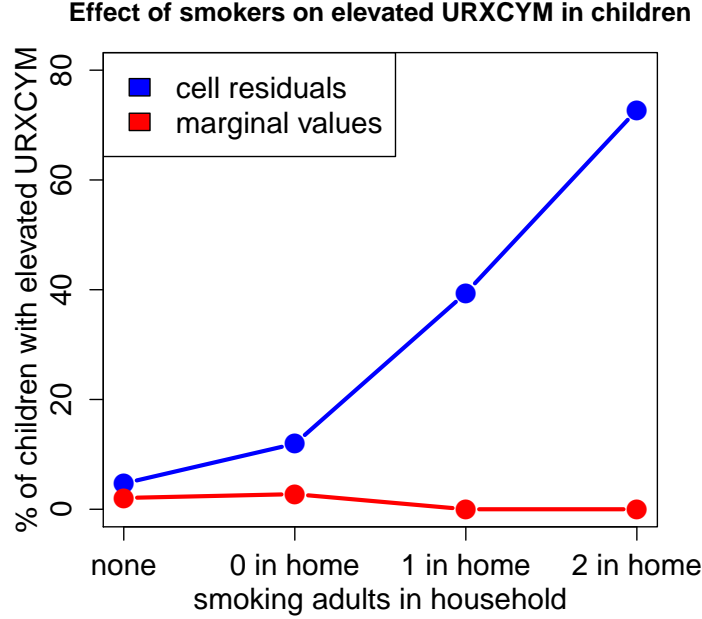


Figure 7: The blue curve shows the percentage of elevated URXYM cell residuals in function of the smoking status of adult family members. The red curve shows the percentage of elevated marginal URXYM values.

The example shows that the effect of exposing children to tobacco smoke could be underestimated when only performing univariate analyses on biomarkers. This illustrates that cell residuals obtained by cellFlagger may add valuable information to a dataset.

## 6 Conclusion

The proposed cellFlagger method is the first to detect cellwise outliers based on robust estimates of location and covariance. It is also a major component of the detection-imputation (DI) algorithm that computes such cellwise robust estimates. Note that both methods can deal with missing values in the data, since these are imputed along the way.

The performance of cellFlagger and DI was illustrated by simulation. A real example illustrated that the common medical practice of comparing individual biomarkers to their tolerance limits can benefit from the use of cellwise residuals.

**Software availability.** A zip file with the R code as well as the data of the example and a

script reproducing its analysis can be downloaded from the website <http://wis.kuleuven.be/statdatascience/robust/software>. At a later stage the code will be made available in the R package *cellWise* on CRAN.

**Acknowledgement.** This research was funded by projects of Internal Funds KU Leuven.

## References

- Agostinelli, C., A. Leung, V. J. Yohai, and R. H. Zamar (2015). Robust estimation of multivariate location and scatter in the presence of cellwise and casewise contamination. *TEST* 24, 441–461.
- Alqallaf, F., S. Van Aelst, V. J. Yohai, and R. H. Zamar (2009). Propagation of outliers in multivariate data. *The Annals of Statistics* 37, 311–331.
- Chandola, V., A. Banerjee, and V. Kumar (2009). Anomaly detection: A survey. *ACM Computing Surveys* 41, 1–58.
- Chen, M., S. G. Carmella, C. Sipe, J. Jensen, X. Luo, C. T. Le, S. E. Murphy, N. L. Benowitz, F. J. McClernon, R. Vandrey, S. S. Allen, R. Denlinger-Apte, P. M. Cinciripini, A. A. Strasser, M. alAbsi, J. D. Robinson, E. C. Donny, D. Hatsukami, and S. S. Hecht (2019). Longitudinal stability in cigarette smokers of urinary biomarkers of exposure to the toxicants acrylonitrile and acrolein. *PLOS ONE* 14(1), 1–13.
- Croux, C. and V. Öllerer (2016). Robust and sparse estimation of the inverse covariance matrix using rank correlation measures. In C. Agostinelli, A. Basu, P. Filzmoser, and D. Mukherjee (Eds.), *Recent Advances in Robust Statistics: Theory and Applications*, New Delhi, pp. 35–55. Springer India.
- Danilov, M. (2010). *Robust estimation of multivariate scatter in non-affine equivariant scenarios*. Ph. D. thesis, University of British Columbia.
- Danilov, M., V. J. Yohai, and R. H. Zamar (2012). Robust estimation of multivariate

- location and scatter in the presence of missing data. *Journal of the American Statistical Association* 107, 1178–1186.
- Debruyne, M., S. Höppner, S. Serneels, and T. Verdonck (2019). Outlyingness: Which variables contribute most? *Statistics and Computing* 29, 707–723.
- Efron, B., T. Hastie, I. Johnstone, and R. Tibshirani (2004). Least angle regression. *The Annals of Statistics* 32, 407–499.
- Farcomeni, A. (2014). Robust constrained clustering in presence of entry-wise outliers. *Technometrics* 56(1), 102–111.
- Farcomeni, A. and A. Leung (2019). *Package snipEM: Snipping Methods for Robust Estimation and Clustering*. CRAN, R package version 1.0.1.
- Gnanadesikan, R. and J. R. Kettenring (1972). Robust estimates, residuals, and outlier detection with multiresponse data. *Biometrics* 28, 81–124.
- Hastie, T. and B. Efron (2015). *Package lars: Least Angle Regression, Lasso and Forward Stagewise*. CRAN, R package version 1.2.
- Higham, N. J. (2002). Computing the nearest correlation matrix - a problem from finance. *IMA Journal of Numerical Analysis* 22, 329–343.
- Leung, A., M. Danilov, V. Yohai, and R. Zamar (2019). *Package GSE: Robust Estimation in the Presence of Cellwise and Casewise Contamination and Missing Data*. CRAN, R package version 4.2.
- Leung, A., V. Yohai, and R. Zamar (2017). Multivariate location and scatter matrix estimation under cellwise and casewise contamination. *Computational Statistics & Data Analysis* 111, 59–76.
- Little, R. and D. Rubin (1987). *Statistical Analysis with Missing Data*. New York: Wiley-Interscience.
- Maronna, R., D. Martin, V. Yohai, and M. Salibián-Barrera (2019). *Robust Statistics: Theory and Methods, Second Edition*. New York: Wiley.

- NHANES (2019). National Health and Nutrition Examination Survey Data. Hyattsville, MD: U.S. Department of Health and Human Services, Centers for Disease Control and Prevention. <https://wwwn.cdc.gov/nchs/nhanes/>.
- Öllerer, V. and C. Croux (2015). Robust high-dimensional precision matrix estimation. In K. Nordhausen and S. Taskinen (Eds.), *Modern Nonparametric, Robust and Multivariate Methods: Festschrift in Honour of Hannu Oja*, pp. 325–350. Cham: Springer International Publishing.
- Petersen, K. B. and M. S. Pedersen (2012). *The Matrix Cookbook*. Technical University of Denmark.
- Raymaekers, J. and P. J. Rousseeuw (2019). Fast robust correlation for high-dimensional data. *Technometrics*, published online, doi 10.1080/00401706.2019.1677270.
- Raymaekers, J., P. J. Rousseeuw, W. Van den Bossche, and M. Hubert (2019). *Package cellWise: Analyzing Data with Cellwise Outliers*. CRAN, R package version 2.2.0.9000.
- Rousseeuw, P. J. and C. Croux (1993). Alternatives to the median absolute deviation. *Journal of the American Statistical Association* 88, 1273–1283.
- Rousseeuw, P. J. and W. Van den Bossche (2018). Detecting deviating data cells. *Technometrics* 60, 135–145.
- Tarr, G., S. Mller, and N. Weber (2016). Robust estimation of precision matrices under cellwise contamination. *Computational Statistics & Data Analysis* 93, 404–420.
- Tibshirani, R. (1996). Regression shrinkage and selection via the lasso. *Journal of the Royal Statistical Society Series B* 58, 267–288.
- Unwin, A. (2019). Multivariate outliers and the O3 plot. *Journal of Computational and Graphical Statistics*, to appear.
- Van Aelst, S., E. Vandervieren, and G. Willems (2011). Stahel-Donoho estimators with cellwise weights. *Journal of Statistical Computation and Simulation* 81(1), 1–27.

## A Supplementary Material

### A.1 Proof of Proposition 2

*Proof.* We first split up the relevant matrices in blocks. Denote

$$\Sigma^{-1} = \begin{bmatrix} \Sigma_{11}^* & \Sigma_{12}^* \\ \Sigma_{21}^* & \Sigma_{22}^* \end{bmatrix} \quad \text{and} \quad \Sigma^{-1/2} = \begin{bmatrix} \tilde{\Sigma}_{11} & \tilde{\Sigma}_{12} \\ \tilde{\Sigma}_{21} & \tilde{\Sigma}_{22} \end{bmatrix}.$$

Let the  $k$ -variate  $\hat{\theta}$  be the solution to the ordinary least squares regression problem

$$\operatorname{argmin}_{\theta} \|\Sigma^{-1/2}(z - \mu) - (\Sigma^{-1/2})_{\cdot 1} \theta\|_2^2$$

where  $(\Sigma^{-1/2})_{\cdot 1}$  denotes the first  $k$  columns of the matrix  $\Sigma^{-1/2}$ .

Then we know that

$$\begin{aligned} \hat{\theta} &= \left( \begin{bmatrix} \tilde{\Sigma}_{11} \\ \tilde{\Sigma}_{21} \end{bmatrix}' \begin{bmatrix} \tilde{\Sigma}_{11} \\ \tilde{\Sigma}_{21} \end{bmatrix} \right)^{-1} \begin{bmatrix} \tilde{\Sigma}_{11} \\ \tilde{\Sigma}_{21} \end{bmatrix}' \Sigma^{-1/2}(z - \mu) \\ &= (\Sigma_{11}^*)^{-1} \begin{bmatrix} \tilde{\Sigma}_{11} \\ \tilde{\Sigma}_{21} \end{bmatrix}' \Sigma^{-1/2}(z - \mu). \end{aligned}$$

Now observe that

$$\begin{aligned} z_1 - \hat{\theta} &= z_1 - (\Sigma_{11}^*)^{-1} \begin{bmatrix} \tilde{\Sigma}_{11} \\ \tilde{\Sigma}_{21} \end{bmatrix}' \Sigma^{-1/2}(z - \mu) \\ &= z_1 - (\Sigma_{11}^*)^{-1} [\Sigma_{11}^* \ \Sigma_{12}^*] [z_1 - \mu_1 \ z_2 - \mu_2] \\ &= z_1 - [I_k \ (\Sigma_{11}^*)^{-1} \Sigma_{12}^*] [z_1 - \mu_1 \ z_2 - \mu_2] \\ &= z_1 - (z_1 - \mu_1) - (\Sigma_{11}^*)^{-1} \Sigma_{12}^* (z_2 - \mu_2) \\ &= \mu_1 + \Sigma_{12} \Sigma_{22}^{-1} (z_2 - \mu_2) \end{aligned}$$

where the last equality follows from  $-(\Sigma_{11}^*)^{-1} \Sigma_{12}^* = \Sigma_{12} \Sigma_{22}^{-1}$  iff  $-\Sigma_{12}^* \Sigma_{22} = \Sigma_{11}^* \Sigma_{12}$  iff  $[\Sigma_{11}^* \ \Sigma_{12}^*] [\Sigma_{12} \Sigma_{22}]' = 0$  which follows from  $\Sigma^{-1} \Sigma = I$ .  $\square$

### A.2 Proof of Proposition 3

*Proof.* We will use the notation  $\hat{\theta}_1 = \operatorname{argmin}_{\theta_1} \|\Sigma^{-1/2}(z - \mu) - (\Sigma^{-1/2})_{\cdot 1} \theta_1\|_2^2$  for the OLS fit, and  $\text{RSS}_k = \|\Sigma^{-1/2}(z - \mu) - (\Sigma^{-1/2})_{\cdot 1} \hat{\theta}_1\|_2^2$ .

### Part 1.

For  $k = d$  we know from (1) that  $\text{RSS}_d = 0$ . Now let  $1 \leq k \leq d - 1$ . We want to show that  $\text{RSS}_k = (\mathbf{z}_2 - \boldsymbol{\mu}_2)' \boldsymbol{\Sigma}_{22}^{-1} (\mathbf{z}_2 - \boldsymbol{\mu}_2)$ . Let  $\hat{\boldsymbol{\theta}} := [\hat{\boldsymbol{\theta}}_1' \ 0 \ \dots \ 0]'$  be the  $d$ -variate vector with coefficients  $\hat{\boldsymbol{\theta}}_1$  followed by  $d - k$  zeroes.

We now have that

$$\begin{aligned} \text{RSS}_k &= \|\boldsymbol{\Sigma}^{-1/2}(\mathbf{z} - \boldsymbol{\mu}) - (\boldsymbol{\Sigma}^{-1/2})_{\cdot 1} \hat{\boldsymbol{\theta}}_1\|_2^2 \\ &= \|\boldsymbol{\Sigma}^{-1/2}(\mathbf{z} - \boldsymbol{\mu}) - \boldsymbol{\Sigma}^{-1/2} \hat{\boldsymbol{\theta}}\|_2^2 \\ &= (\mathbf{z} - \boldsymbol{\mu} - \hat{\boldsymbol{\theta}})' \boldsymbol{\Sigma}^{-1} (\mathbf{z} - \boldsymbol{\mu} - \hat{\boldsymbol{\theta}}) \\ &= [\mathbf{z}_1 - \boldsymbol{\mu}_1 - \hat{\boldsymbol{\theta}}_1 \quad \mathbf{z}_2 - \boldsymbol{\mu}_2]' \boldsymbol{\Sigma}^{-1} [\mathbf{z}_1 - \boldsymbol{\mu}_1 - \hat{\boldsymbol{\theta}}_1 \quad \mathbf{z}_2 - \boldsymbol{\mu}_2] . \end{aligned}$$

Following page 47 of Petersen and Pedersen (2012) we can write  $\boldsymbol{\Sigma}^{-1} = \mathbf{A} \mathbf{B} \mathbf{A}'$  with

$$\mathbf{A} := \begin{bmatrix} \mathbf{I} & \mathbf{0} \\ -\boldsymbol{\Sigma}_{22}^{-1} \boldsymbol{\Sigma}_{21} & \mathbf{I} \end{bmatrix} \quad \text{and} \quad \mathbf{B} := \begin{bmatrix} \mathbf{C}_1^{-1} & \mathbf{0} \\ \mathbf{0} & \boldsymbol{\Sigma}_{22}^{-1} \end{bmatrix}$$

where  $\mathbf{C}_1 := \boldsymbol{\Sigma}_{11} - \boldsymbol{\Sigma}_{12} \boldsymbol{\Sigma}_{22}^{-1} \boldsymbol{\Sigma}_{21}$ . We now have that

$$\begin{aligned} [\mathbf{z}_1 - \boldsymbol{\mu}_1 - \hat{\boldsymbol{\theta}}_1 \quad \mathbf{z}_2 - \boldsymbol{\mu}_2]' \mathbf{A} &= [\mathbf{z}_1 - \boldsymbol{\mu}_1 - \hat{\boldsymbol{\theta}}_1 - (\mathbf{z}_2 - \boldsymbol{\mu}_2) \boldsymbol{\Sigma}_{22}^{-1} \boldsymbol{\Sigma}_{21} \quad \mathbf{z}_2 - \boldsymbol{\mu}_2]' \\ &= [\mathbf{0} \quad \mathbf{z}_2 - \boldsymbol{\mu}_2]' \end{aligned}$$

using the result of Proposition 2. Therefore,

$$\begin{aligned} \text{RSS}_k &= [\mathbf{z}_1 - \boldsymbol{\mu}_1 - \hat{\boldsymbol{\theta}}_1 \quad \mathbf{z}_2 - \boldsymbol{\mu}_2]' \boldsymbol{\Sigma}^{-1} [\mathbf{z}_1 - \boldsymbol{\mu}_1 - \hat{\boldsymbol{\theta}}_1 \quad \mathbf{z}_2 - \boldsymbol{\mu}_2] \\ &= [\mathbf{0} \quad \mathbf{z}_2 - \boldsymbol{\mu}_2]' \mathbf{B} [\mathbf{0} \quad \mathbf{z}_2 - \boldsymbol{\mu}_2] \\ &= (\mathbf{z}_2 - \boldsymbol{\mu}_2)' \boldsymbol{\Sigma}_{22}^{-1} (\mathbf{z}_2 - \boldsymbol{\mu}_2) . \end{aligned}$$

### Part 2.

We will now show that the differences in RSS follow a  $\chi^2(1)$  distribution, that is  $\Delta_k := \text{RSS}_{k-1} - \text{RSS}_k \sim \chi^2(1)$  assuming that  $\mathbf{z} = [\mathbf{z}_1' \ \mathbf{z}_2']'$  is multivariate Gaussian with mean  $\boldsymbol{\mu}$  and covariance matrix  $\boldsymbol{\Sigma}$ . For  $k = 0$  we set by convention  $\hat{\boldsymbol{\theta}} := \mathbf{0}$  and  $\text{RSS}_0 := \|\boldsymbol{\Sigma}^{-1/2}(\mathbf{z} - \boldsymbol{\mu})\|_2^2$ .

We show the result for  $k = 1$  as the subsequent steps are analogous. The reasoning below is similar to Appendix A.2 of Danilov (2010) where the cells were not yet ranked

from most to least outlying. As in Part 1 of the proof we can write  $\Sigma^{-1} = \mathbf{A}\mathbf{B}\mathbf{A}'$  with

$$\mathbf{A} = \begin{bmatrix} 1 & \mathbf{0} \\ -\Sigma_{22}^{-1}\Sigma_{21} & \mathbf{I} \end{bmatrix} \quad \text{and} \quad \mathbf{B} = \begin{bmatrix} C_1^{-1} & \mathbf{0} \\ \mathbf{0} & \Sigma_{22}^{-1} \end{bmatrix}$$

where this time  $C_1 = \Sigma_{11} - \Sigma_{12}\Sigma_{22}^{-1}\Sigma_{21}$  is a scalar. We can then write

$$\begin{aligned} \text{RSS}_0 &= (\mathbf{z} - \boldsymbol{\mu})' \Sigma^{-1} (\mathbf{z} - \boldsymbol{\mu}) \\ &= (\mathbf{z} - \boldsymbol{\mu})' \mathbf{A}\mathbf{B}\mathbf{A}' (\mathbf{z} - \boldsymbol{\mu}) \\ &= [z_1 - \mu_1 - (\mathbf{z}_2 - \boldsymbol{\mu}_2)\Sigma_{22}^{-1}\Sigma_{21} \quad \mathbf{z}_2 - \boldsymbol{\mu}_2]' \mathbf{B} [z_1 - \mu_1 - (\mathbf{z}_2 - \boldsymbol{\mu}_2)\Sigma_{22}^{-1}\Sigma_{21} \quad \mathbf{z}_2 - \boldsymbol{\mu}_2] \\ &= ((z_1 - \mu_1^*)/\sigma_1^*)^2 + (\mathbf{z}_2 - \boldsymbol{\mu}_2)' \Sigma_{22}^{-1} (\mathbf{z}_2 - \boldsymbol{\mu}_2) \\ &= ((z_1 - \mu_1^*)/\sigma_1^*)^2 + \text{RSS}_1 \end{aligned}$$

where  $\mu_1^* := \mu_1 + (\mathbf{z}_2 - \boldsymbol{\mu}_2)\Sigma_{22}^{-1}\Sigma_{21}$  and  $\sigma_1^* := \sqrt{C_1}$ . So we obtain

$$\Delta_1 = \text{RSS}_0 - \text{RSS}_1 = ((z_1 - \mu_1^*)/\sigma_1^*)^2$$

and this is the square of a standard Gaussian variable since  $z_1 - \mu_1^*$  is Gaussian with expectation 0 and standard deviation  $\sigma_1^*$ . We thus have  $\Delta_1 \sim \chi^2(1)$ .  $\square$

### A.3 Implementation of the cellFlagger algorithm

The LAR component of cellFlagger is a regression of  $\tilde{\mathbf{Y}}$  on  $\dot{\mathbf{X}}$  as defined in the paper. Since this regression has no intercept and we need to preserve the column scaling in  $\dot{\mathbf{X}}$ , we run the function `lars::lar` with the options `intercept=F` and `normalize=F`.

For the imputations in Proposition 2 and the RSS in Proposition 3 we require the OLS fits  $\hat{\boldsymbol{\theta}}_A$  minimizing  $\|\Sigma^{-1/2}(\mathbf{z} - \boldsymbol{\mu}) - (\Sigma^{-1/2})_A \boldsymbol{\theta}_1\|_2^2$  where  $A$  is the set of active predictor variables in every step of LAR. Fortunately, these can be obtained without significant additional computation time because each step of LAR already carries out the QR decomposition of  $(\dot{\mathbf{X}}_A)' \dot{\mathbf{X}}_A$  where  $\dot{\mathbf{X}}_A$  is the submatrix of  $\dot{\mathbf{X}}$  consisting of the columns in  $A$ . The resulting OLS regression vectors  $\hat{\boldsymbol{\beta}}_A$  obtained by LAR (which contain zeroes for the inactive variables) are then easily rescaled to  $\hat{\boldsymbol{\theta}}_A = \mathbf{W}^{-1} \hat{\boldsymbol{\beta}}_A$ .

## A.4 Description of the initial estimator DDCW

The Detection-Imputation (DI) method of Section 3.2 needs initial cellwise robust estimates  $\hat{\boldsymbol{\mu}}^0$  and  $\hat{\boldsymbol{\Sigma}}^0$  of location and covariance. One option is to insert the 2SGS estimator of Leung et al. (2017). We also developed a different initial estimator called DDCW, which we describe here. Its steps are:

1. Drop variables with too many missing values or zero median absolute deviation, and continue with the remaining columns.
2. Run the DetectDeviatingCells (DDC) method (Rousseeuw and Van den Bossche, 2018) with the constraint that no more than  $n_{maxCol}$  cells are flagged in any variable. DDC also rescales the variables, and may delete some cases. Continue with the remaining imputed and rescaled cases denoted as  $\mathbf{z}_i$ .
3. Project the  $\mathbf{z}_i$  on the axes of their principal components, yielding the transformed data points  $\tilde{\mathbf{z}}_i$ .
4. Compute the wrapped location  $\hat{\boldsymbol{\mu}}_w$  and covariance matrix  $\hat{\boldsymbol{\Sigma}}_w$  (Raymaekers and Rousseeuw, 2019) of these  $\tilde{\mathbf{z}}_i$ . Next, compute the temporary points  $\mathbf{u}_i = (u_{i1}, \dots, u_{id})$  given by  $u_{ij} = \max\{\min\{\tilde{z}_{ij} - (\hat{\boldsymbol{\mu}}_w)_j, 2\}, -2\}$ . Then remove all cases for which the squared robust distance  $RD^2(i) = \mathbf{u}_i' \hat{\boldsymbol{\Sigma}}_w^{-1} \mathbf{u}_i$  exceeds  $\chi_{d,q}^2 \text{median}_h(RD^2(h)) / \chi_{d,0.5}^2$ .
5. Project the remaining  $\tilde{\mathbf{z}}_i$  on the eigenvectors of  $\hat{\boldsymbol{\Sigma}}_w$  and again compute a wrapped location and covariance matrix.
6. Transform these estimates back to the original coordinate system of the imputed data, and undo the scaling. This yields the estimates  $\hat{\boldsymbol{\mu}}^0$  and  $\hat{\boldsymbol{\Sigma}}^0$ .

Note that DDCW can handle missing values since the DDC method in step 2 imputes them.

The reason for the truncation in the rejection rule in step 4 is that otherwise the robust distance RD could be inflated by an outlying cell. Overall, DDCW tends to remove the casewise outliers which are outlying due to strong deviations from the covariance structure. These are typically rows which cannot be shifted towards the majority of the data without



changing a large number of cells, and therefore we keep them out of the iteration steps of the subsequent DI algorithm.

## A.5 More on the DI algorithm

**D-step.** The D-step imposes a maximum on the number of flagged cells in a row, namely  $n \text{ maxCol}$  where  $\text{maxCol}$  is set to 25% by default. Since all missing values (NA's) are automatically flagged, the algorithm would not be able to run if there are too many NA's in a column. In practice, the algorithm starts by setting variables with too many NA's aside and giving a message about this.

**Updating  $\hat{\mu}$  and  $\hat{\Sigma}$  in the I-step.** We re-estimate the center as  $\hat{\mu}^t$  which is the mean of the dataset with its imputed cells. For computing  $\hat{\Sigma}^t$  the formula of the M-step is more complicated: it is not just the covariance matrix of the imputed data, since this would underestimate the true variability. Therefore a bias correction is added. This bias correction depends on which cells were imputed, and can therefore be different for every row of the data. Suppose the first row  $\mathbf{z}_1$  has an imputed part  $\mathbf{z}_{1i}$  and an untouched part  $\mathbf{z}_{1u}$ , then the bias correction matrix from that row is

$$B_{ii} = \frac{1}{n} \hat{\Sigma}_{uu}^{t-1} - \frac{1}{n} \hat{\Sigma}_{iu}^{t-1} (\Sigma_{uu}^{t-1})^{-1} \Sigma_{ui}^{t-1} .$$

This correction term is known to remove the bias when the data is uncontaminated multivariate Gaussian with missing values generated completely at random (MCAR), that is, independent of both the observed cells as well as the values the missing cells had before they became unavailable. Also in our simulations with contaminated data this bias correction turned out to improve the results.

## A.6 Simulation with both cellwise and casewise outliers

We now run a simulation in which the data are contaminated by 10% of cellwise outliers generated as in the paper, plus 10% of rowwise outliers. In this particular setting “rowwise outliers” refers to rows in which all cells are contaminated in the same way as before, that is, rows with  $d$  cellwise outliers. We generate these outlying rows by the formula  $\mathbf{v} = \gamma d \sqrt{d} \mathbf{u}' / \text{MD}(\mathbf{u}, \boldsymbol{\mu}, \boldsymbol{\Sigma})$  where  $\mathbf{u}$  is the eigenvector of  $\boldsymbol{\Sigma}$  with smallest eigenvalue. This corresponds to the cellwise formula of Subsection 2.3 in which the indices of the outlying cells  $K = \{j(1), \dots, j(k)\}$  are replaced by  $K = \{1, \dots, d\}$ . Next, we replace 10% of the rows by  $\mathbf{v}$ , and afterward sample the positions of the cellwise outliers from the remaining 90% of the rows. The results are shown in Figures 8 and 9. They look qualitatively similar to those in Figures 4 and 5 in the paper.

ALYZ, 10% cells & 10% cases,  $d = 10$       A09, 10% cells & 10% cases,  $d = 10$

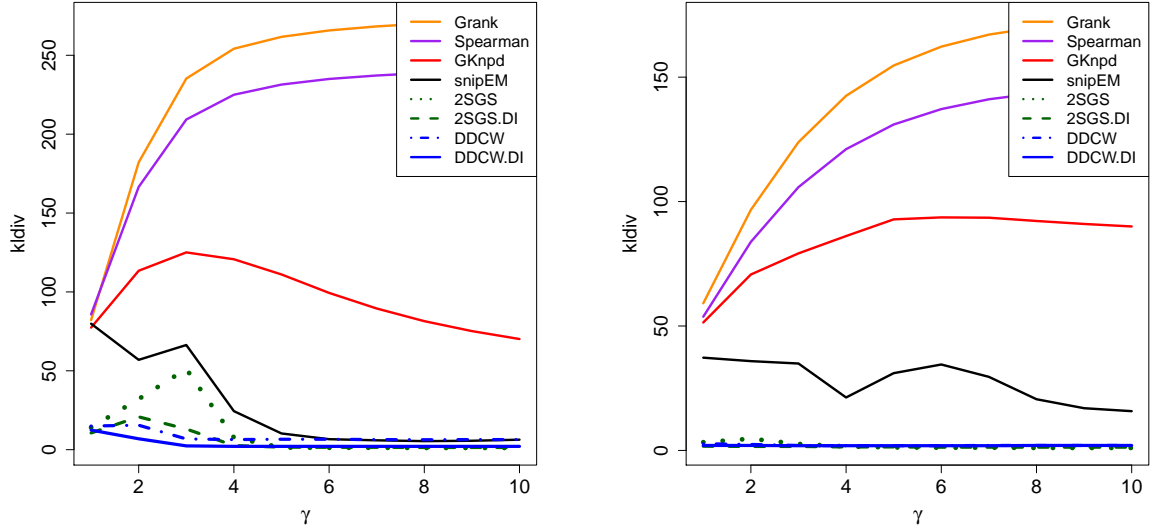
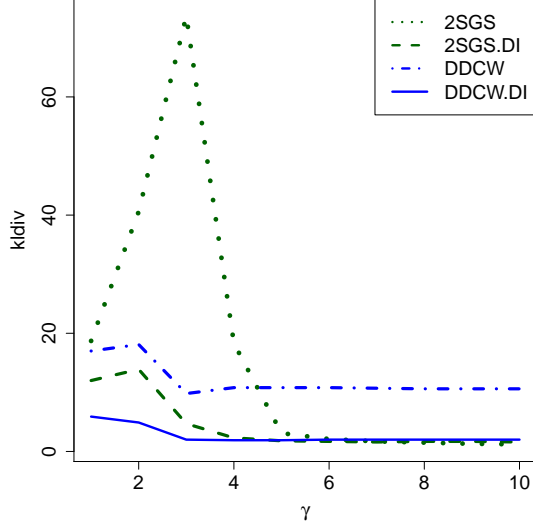
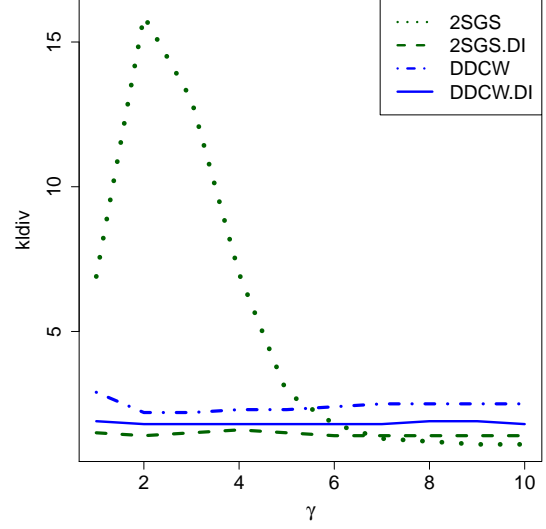


Figure 8: Kullback-Leibler divergence of covariance matrices for  $d = 10$  and  $n = 100$ .

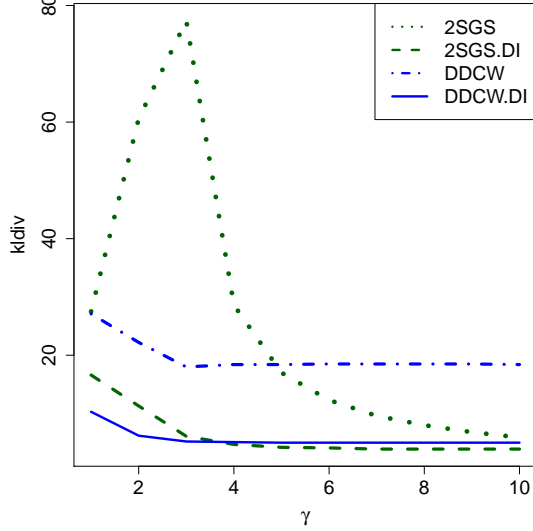
ALYZ, 10% cells & 10% cases,  $d = 20$



A09, 10% cells & 10% cases,  $d = 20$



ALYZ, 10% cells & 10% cases,  $d = 40$



A09, 10% cells & 10% cases,  $d = 40$

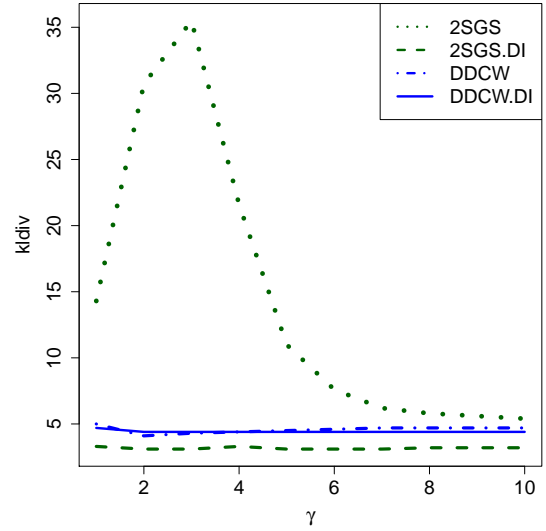


Figure 9: Kullback-Leibler divergence of covariance matrices for  $d = 20$  and  $n = 400$  (top panels) and for  $d = 40$  and  $n = 800$  (bottom panels).

## A.7 List of volatile organic compounds

The volatile organic compounds (VOC's) analyzed in Section 5 are listed below.

Variable Name	VOC name
URX2MH	2-Methylhippuric acid
URX34M	3- and 4-Methylhippuric acid
URXAAM	N-Acetyl-S-(2-carbamoylethyl)-L-cysteine
URXAMC	N-Acetyl-S-(N-methylcarbamoyl)-L-cysteine
URXATC	2-Aminothiazoline-4-carboxylic acid
URXBMA	N-Acetyl-S-(benzyl)-L-cysteine
URXCEM	N-Acetyl-S-(2-carboxyethyl)-L-cysteine
URXCYM	N-Acetyl-S-(2-cyanoethyl)-L-cysteine
URXDHB	N-Acetyl-S-(3,4-dihydroxybutyl)-L-cysteine
URXHP2	N-Acetyl-S-(2-hydroxypropyl)-L-cysteine
URXHPM	N-Acetyl-S-(3-hydroxypropyl)-L-cysteine
URXIPM3	N-Acetyl-S-(4-hydroxy-2-methyl-2-butenyl)-L-cysteine
URXMAD	Mandelic acid
URXMB3	N-Acetyl-S-(4-hydroxy-2-butenyl)-L-cysteine
URXPHG	Phenylglyoxylic acid
URXPMM	N-Acetyl-S-(3-hydroxypropyl-1-methyl)-L-cysteine